厚生労働省科学研究費補助金（難治性疾患克服研究事業）
分担研究報告書

種々の原因による水疱性角膜症に対する角膜内皮移植術の成績

研究分担者　島﨑 潤　東京歯科大学市川総合病院眼科

研究要旨：フックス角膜変性症に対する角膜内皮移植術(DSAEK)の術後成績を、アルゴンレーザー虹彩切開術後、および白内障術後の水疱性角膜症と比較した。術前の眼軸長、白内障合併の有無、角膜浮腫の程度などには３群間で差がみられたが、術後成績にはどの群でも差がなかった。結論として、どの原因による水疱性角膜症に対しても、適切な手術手技を工夫することでほぼ同等の結果を得ることができると考えられた。

A. 研究目的

フックス内皮変性症を始めとする水疱性角膜症に対しては、Descemet's stripping and automated endothelial keratoplasty (DSAEK)がスタンダードな手術法として取り入れられている。本術式の成績については、欧米を中心に数多く報告されているが、欧米とわが国では原因疾患や人種による解剖学的特性が異なっており、その成績がそのまま当てはまるかは不明である。今回の研究では、わが国における水疱性角膜症の３大原因疾患について DSAEK の成績を比較検討した。

B. 研究方法

東京歯科大学眼科で DSAEK を行った 103 眼を原因疾患別に３つに分けて術後成績をレトロスペクティブに検討した。疾患としては、フックス角膜変性症（FED 群、２１眼）、アルゴンレーザー角膜切開術後(ALI 群、５４眼)、および白内障術後(PBK 群、２８眼)であった。

C. 研究結果

術前の状態では、ALI 群が他の２群に比べて有意に眼軸長が短く、強度の角膜浮腫、白内障、虹彩癒着、散瞳不良の合併が多かった。ALI 群の３７眼、FED 群の１３眼で白内障と DSAEK の同時手術が施行された。術後の矯正視力、等価球面度数、惹起乱視度数、角膜乱視、内皮細胞密度、術中及び術後合併症の頻度は３群間で有意差がなかった。

D. 考察

ALI 群の術前の状態は、DSAEK 手術をより困難にする要因を多く含んでいた。これは本疾患がアジア人特有の小さな眼に合併しやすいこと、およびわが国ではドナー角膜の供給が不十分なことから、移植手術のタイミングが遅れがちなことが関係していると考えられた。しかしながら、DSAEK 手術方法の工夫により、これらの要因をカバーすることが多くの場合可能であり、FED 群や PBK 群と同等の術後成績が得られた。

E. 結論

わが国で水疱性角膜症の多数を占めるアルゴンレーザー虹彩切開術後の水疱性角膜症は、術前の状態が他の原因に比べてより重篤であるにもかかわらず、DSAEK 術後の成績にはフックス角膜変性症などと比べて大きな差はなかった。

G. 研究発表

1. 論文発表

Hirayama M, Yamaguchi T, Satake Y, and Shimazaki J. Surgical Outcome of Descemet's Stripping Automated Endothelial Keratoplasty for Bullous Keratopathy Secondary to Argon Laser Iridotomy. Graefe's Archive for Clinical and Experimental Ophthalmology (in press)

2. 学会発表

なし

H. 知的財産権の出願、登録状況

該当するものなし

厚生労働省科学研究費補助金（難治性疾患克服研究事業）
分担研究報告書

研究分担者　小林　顕、横川英明、杉山和久　所属施設　金沢大学

研究発表

1.　論文発表

Yoshiro Mawatari, Akira Kobayashi, Hideaki Yokogawa, and Kazuhisa Sugiyama. Intraocular Pressure After Descemet's Stripping and Non-Descemet's Stripping Automated Endothelial Keratoplasty. Japanese Journal of Ophthalmology. 2011 Mar;55(2):98-102.

Kobayashi A, Yokogawa H, Sugiyama K. In vivo laser confocal microscopy findings of Thygeson superficial punctate keratitis. Cornea. 2011 Jun;30(6):675-80.

Kobayashi A, Yokogawa H, Higashide T, Nitta K, Sugiyama K. Clinical Significance of Owl Eye Morphologic Features by In Vivo Laser Confocal Microscopy in Patients with Cytomegalovirus Corneal Endotheliitis. Am J Ophthalmol. 2011 Oct 24. in printing

Akira Kobayashi, Hideaki Yokogawa, and Kazuhisa Sugiyama. Clinical Evaluation of a New Donor Graft Inserter for Descemet's Stripping Automated Endothelial Keratoplasty. Ophthalmic surgery, lasers & imaging. 2011 in printing

Toshinori Masaki, Akira Kobayashi, Hideaki Yokogawa,Yoshiaki Saito, and Kazuhisa Sugiyama. Clinical Evaluation of non-Descemet's Stripping Automated Endothelial Keratoplasty (nDSAEK). Japanese Journal of Ophthalmology. 2011 in printing

2.　学会発表

小林　顕、横川英明、杉山和久．ヒト角膜におけるデスメ膜ドナー採取方法についての検討．角膜カンファランス 2011　東京 2011/2/17-2/19

正木利憲、小林　顕、横川英明、杉山和久．アルゴンレーザー虹彩切開術後水疱性角膜症における nDSAEK の術後成績．角膜カンファランス 2011　東京　2011/2/17-2/19

横川英明、小林顕、杉山和久．サイトメガロウイルス角膜内皮炎の生体レーザー共焦点顕微鏡所見．角膜カンファランス2011　東京　2011/2/17-2/19

山崎奈津子、横川英明、小林顕、石橋康久、及川陽三郎、所正治、杉山和久．角膜カンファランス2011　東京　2011/2/17-2/19

八田裕貴子、横川英明、小林顕、鳥崎真人、杉山和久．特異な上皮下混濁を合併したプレデスメジストロフィの共焦点顕微鏡所見．角膜カンファランス2011　東京　2011/2/17-2/19

中野愛、横川英明、小林顕、杉山和久．落屑症候群起因の水疱性角膜症に対する角膜内皮移植術の成績．角膜カンファランス2011　東京　2011/2/17-2/19

（発表誌名巻号・頁・発行年等も記入）

H．知的財産権の出願・登録状況
（予定を含む。）

特になし。

研究成果の刊行に関する一覧表

研究成果の刊行に関する一覧表

雑誌

発表者氏名	論文タイトル名	発表誌名	巻号	ページ	出版年
Hatou S, Shimmura S, Shimazaki J, Usui T, Amano S, Yokogawa H, Kobayashi A, Zheng X, Shiraishi A, Ohashi Y, Inatomi T, Tsubota K.	Mathematical projection model of visual loss due to Fuchs corneal dystrophy.	Invest Ophthalmol Vis Sci.	52(11)	7888-93	2011
Hatou S.	Hormonal regulation of Na^+-/K^+-Dependent ATPase Activity and Pump Function in Corneal Endothelial Cells.	Cornea.	30 Suppl 1	S60-6.	2011
Zheng X, Shiraishi A, Okuma S, Mizoue S, Goto T, Kawasaki S, Uno T, Miyoshi T, Ruggeri A, Ohashi Y.	In vivo confocal microscopic evidence of keratopathy in patients with pseudoexfoliation syndrome.	Invest Ophthalmol Vis Sci.	52(3)	1755-61.	2011
Yamazoe K, Yamaguchi T, Hotta K, Satake Y, Konomi K, Den S, Shimazaki J.	Outcomes of cataract surgery in eyes with a low corneal endothelial cell density.	J Cataract Refract Surg.	37(12)	2130-6	2011

Hirayama M, Yamaguchi T, Satake Y, Shimazaki J.	Surgical outcome of Descemet's stripping automated endothelial keratoplasty for bullous keratopathy secondary to argon laser iridotomy.	Graefes Arch Clin Exp Ophthalmol.	Jan 28. [Epub ahead of print]		2012
Yoshiro Mawatari, Akira Kobayashi, Hideaki Yokogawa, and Kazuhisa Sugiyama	Intraocular Pressure After Descemet's Stripping and Non-Descemet's Stripping Automated Endothelial Keratoplasty	Japanese Journal of Ophthalmology	55	98-102	2011
Akira Kobayashi, Hideaki Yokogawa, and Kazuhisa Sugiyama	In vivo laser confocal microscopy findings of Thygeson superficial punctate keratitis.	Cornea	30	675-680	2011
Akira Kobayashi, Hideaki Yokogawa, Tomomi Higashide, Koji Nitta, and Kazuhisa Sugiyama	Clinical Significance of Owl Eye Morphologic Features by In Vivo Laser Confocal Microscopy in Patients with Cytomegalovirus Corneal Endotheliitis	American Journal of Ophthalmology	In printing	In printing	2011

研究成果の刊行物・別刷

Mathematical Projection Model of Visual Loss Due to Fuchs Corneal Dystrophy

Shin Hatou,[1] Shigeto Shimmura,[1] Jun Shimazaki,[2] Tomohiko Usui,[3] Shiro Amano,[3] Hideaki Yokogawa,[4] Akira Kobayashi,[4] Xiaodong Zheng,[5] Atsushi Shiraishi,[5] Yuichi Ohashi,[5] Tsutomu Inatomi,[6] and Kazuo Tsubota[1]

Purpose. To devise a mathematical disease classification model for eyes with primary guttata cornea, on the bases of endothelial loss trajectory and probability of advanced disease.

Methods. A series of 1971 patients (3281 eyes), some with and some without guttata corneas, undergoing specular microscopy were retrospectively reviewed. The eyes were classified into four stages; stage 0, without guttae; 1, guttata cornea without edema; 2, mild Fuchs' corneal dystrophy (FCD); and 3, severe FCD, according to clinical records, and patient age and corneal endothelial cell density (ECD) were plotted. Nonparametric density smoothing was used to create a contour map, and a best-fit curve for ECD loss was calculated. The relation between ECD decrease rate and the stages were evaluated.

Results. Endothelial decrease rate in stage 0 was 0.44%/year, which was compatible with that of normal eyes reported in previous studies. Decrease rates of stages 1, 2, and 3 were 0.81%, 2.65%, and 3.08%/ year, respectively. The age-ECD loss curves of 1.40%/year ($ECO_{1.4}$) and 2.00%/year ($ECO_{2.0}$) further divided stage 1 into three subgroups; stage 1a, asymptomatic guttata cornea; 1b, borderline guttata cornea; and 1c, pre-FCD. The $ECO_{2.0}$ cutoff line differentiated eyes with FCD from those without edema with a sensitivity and specificity of >90%. Stage 1c eyes were below $ECO_{2.0}$ and had a decrease rate as high as FCD.

Conclusions. This mathematical model can be used to predict the prognosis of patients with primary guttata cornea. (*Invest Ophthalmol Vis Sci.* 2011;52:7888–7893) DOI:10.1167/iovs.11-8040

From the [1]Department of Ophthalmology, Keio University School of Medicine, Shinjuku, Japan; the [2]Department of Ophthalmology, Tokyo Dental College Ichikawa General Hospital, Tokyo, Japan; the [3]Department of Ophthalmology, Tokyo University School of Medicine, Tokyo, Japan; the [4]Department of Ophthalmology, Kanazawa University School of Medicine, Kanazawa, Japan. the [5]Department of Ophthalmology, Ehime University School of Medicine, Matsuyama, Japan; and the [6]Department of Ophthalmology, Kyoto Prefectural University of Medicine, Kyoto, Japan.

Supported by a grant from the Ministry of Health, Labor and Welfare, Japan. The sponsor or funding organization had no role in the design or conduct of this research.

Submitted for publication June 14, 2011; revised August 8, 2011; accepted August 12, 2011.

Disclosure: **S. Hatou**, None; **S. Shimmura**, None; **J. Shimazaki**, None; **T. Usui**, None; **S. Amano**, None; **H. Yokogawa**, None; **A. Kobayashi**, None; **X. Zheng**, None; **A. Shiraishi**, None; **Y. Ohashi**, None; **T. Inatomi**, None; **K. Tsubota**, None

Corresponding author: Shigeto Shimmura, Department of Ophthalmology, Keio University School of Medicine, 35 Shinanomachi, Shinjuku, Tokyo 160-8582, Japan;shige@sc.itc.keio.ac.jp.

Fuchs' corneal dystrophy (FCD) is a progressive, bilateral corneal dystrophy.[1] There is a progressive loss of corneal endothelial cells with secretion of an abnormally thickened basement membrane, leading to corneal guttae formation.[1] On specular microscopy, these corneal guttae are observed as dark areas.[1,2] As endothelial function deteriorates, corneal edema increases and visual acuity declines,[2] and FCD is a major indication for keratoplasty (corneal transplants) in the United States.[3–5] Although FCD is recognized as a dominantly inherited disorder, females are predisposed to it and develop corneal guttae 2.5 times more frequently than do males, progressing to corneal edema 5.7 times more often than do males.[6] The prevalence of primary guttata cornea and FCD are lower in Japan than in the United States.[7,8] This difference in prevalence is thought to be mainly attributable to the racial difference.[7]

Primary guttata cornea is believed to be a preliminary stage of FCD. Krachmer et al.[6] graded guttata cornea and FCD according to a spread of guttae and reported that there was a positive correlation between age and grade of guttae. However, the exact natural course of guttata cornea, or whether all cases of guttata cornea progress to FCD remains to be determined. A prospective study that follows the decline in endothelial cells density (ECD) with age would be ideal for predicting the natural course of guttata cornea; however, a very long follow-up would be required, and recruiting asymptomatic potential patients is practically impossible, especially in Japan. A retrospective study with a large database and an adequate mathematical model can be used in a similar way to predict the prognosis of patients with guttata cornea. In this report, we retrospectively reviewed age and ECD in a large group of hospital-based patients and evaluated the prevalence of guttae, male:female ratio, and distribution of age and ECD. In addition, we propose a new classification of guttata cornea based on a mathematical model that adequately predicts the prognosis of disease.

Methods

Subjects

Clinical records of outpatients who underwent specular microscopy for corneal endothelial cell counts from January through December 2009 in six hospitals affiliated with the Fuchs' Corneal Dystrophy Study Group of Japan were retrospectively reviewed. The purpose of specular microscopy for those patients were routine examination before ocular surgery, follow-up for corneal diseases that were thought to have little effect on endothelium (such as keratoconus or lattice corneal dystrophy), or follow-up for diagnosed Fuchs' corneal dystrophy. Patients who had a history of trauma, corneal infection, intraocular inflammation, intraocular surgery, or laser iridotomy were excluded from the study. Endothelial photographs were taken at the center of the pupillary area with a noncontact specular microscope (Nonkon Robo F & A; Konan Medical, Nishinomiya, Japan, or EM-3000; Tomey,

Investigative Ophthalmology & Visual Science, October 2011, Vol. 52, No. 11

Nagoya, Japan), and analyses of the photographs were performed with an automatic cell analysis system attached to the microscope. Data concerning patient age, sex, presence of guttae, and ECD were recorded. The eyes were classified into four groups by slit lamp examination according to modified Stocker's classification[9]:

Stage 1: Guttata cornea without the stroma or the epithelium being affected

Stage 2: Permeation of corneal stroma with fluid, edema of epithelium, and bullae formation

Stage 3: Late stages with subepithelial connective tissue formation, vascularization, and scar formation

Other eyes without corneal guttae were classified as stage 0. During the rest of the article, the term Fuchs' corneal dystrophy (FCD) represents stage 2 and 3, since eyes in these stages have symptoms related to corneal edema. The study complied with the Declaration of Helsinki. Approval was granted by the Committee for the Protection of Human Subjects of each hospital.

Mathematical Model of Endothelial Cell Loss Rate

To construct a mathematical model of decrease in endothelial cells, we made the following two assumptions:

1. The ECD at 5 years of age is 3600 cells/mm^2. This is common to all classes.
2. From 5 years of age, the decrease rate (percent/year) of ECD is constant in each class, but different between classes.

Murphy et al.[10] reported that during first 2 years of life ECD decreased rapidly because of corneal growth, and after that the decrease rate slows down to 0.56%/year. The effect of corneal growth on ECD ends at 5 years of age or earlier. To simplify our mathematical model, we assumed that ECD at 5 years of age was common to all classes and regarded this point as the base point of age-ECD curve in our mathematical model. Because the onset of FCD is in adulthood, we believe that this assumption is acceptable. We substituted the mean ECD of normal 5-year-old children (3600 cells/mm^2) in the report of Nucci et al.[11] for the base point. We assumed that the (percentage) decrease rate is dependent on the class, and it is constant in each class from 5 years of age. Based on these assumptions, the following differential equation stands:

$$dE_{(t)}/d(t) = -(D/100) \cdot E_{(t)}$$

$$E_{(t=0)} = 3600$$

where t is age 5 years; $E_{(t)}$ is endothelial cell density at t years (in cells per square millimeter); and D is the decrease rate (percent).

The solution to the differential equation is the following:

$$E_{(t)} = 3600e^{[-(D/100)t]}$$

Using this mathematical model, an age-ECD curve in each class can be drawn by the least-squares method. An age–ECD curve of optimal decrease rate can be drawn as well.

Statistical Analysis

Scatterplotting, analysis of variance (ANOVA), nonparametric density smoothing, age-ECD curve, and other statistical analyses were calculated by or written in commercial software (Excel 2007; Microsoft, Redmond, WA, and JMP 8 software; SAS, Cary, NC). $P < 0.05$ was considered statistically significant.

Results

Characteristics of Patients

Age, sex, and stage of reviewed patients and eyes are presented in Table 1. The prevalence of guttata cornea (stage 1+2+3) was 12.73%. The prevalence of stage 1 was 10.65%, and FCD (stage 2+3) was 2.08%. The male: female ratio in each stage was as follows; 1: 1.03 (stage 0), 1: 1.88 (stage 1), 1: 2.43 (stage 2), and 1: 4.67 (stage 3). Females were more predisposed to stage 1 or FCD than males, and the ratio increased in advanced stages.

Age-ECD Curve of 2.0% Differentiates Fuchs' Dystrophy

Figure 1, left shows the scatterplot between age and ECD for each stage. Nonparametric density smoothing was drawn on the scatterplot (Fig. 1, right), which represents the contour of plot density. The age-ECD curves based on our mathematical model were drawn by the least-squares method. Table 2 shows ECD with sample sizes at 5-year intervals for grades 0 to 3, which enables the mean ECD data of grade 0 to 3 to be compared at various ages.

The decreased rate curve of stage 1 age-ECD was 0.81%, which was closer to that of stage 0 (decrease rate, 0.44%) than that of stage 2 (2.65%) or stage 3 (3.08%). The decrease rate of stage 0 in our study was 0.44%, which is within the range of

Table 1. The Age, Sex, and Stages of Reviewed Patients and Eyes

					Prevalence (%)		
Patient Stage	**Age, y (Mean ± SD)**	**Male (*n*)**	**Female (*n*)**	**Total (*n*)**	**Total**	**Male**	**Female**
0	65.3 ± 16.2	848	872	1720			
1	68.5 ± 14.3	73	137	210	10.65	7.84	13.17
2	70.3 ± 10.6	7	17	24	1.22] 2.08	0.75] 1.07	1.63] 2.98
3	75.1 ± 12.4	3	14	17	0.86	0.32	1.35
Total	66.6 ± 15.4	931	1040	1971	12.73	8.91	16.15

Eye Stage	**Male (*n*)**	**Female (*n*)**	**Total (*n*)**
0	1426	1483	2909
1	103	205	308
2	13	28	41
3	5	18	23
Total	1547	1734	3281

Prevalence of FCD was calculated as sum of stage 2 and 3. In this table, if a patient had eyes in different stages, then he or she was classified in the severer of the stages between the eyes.

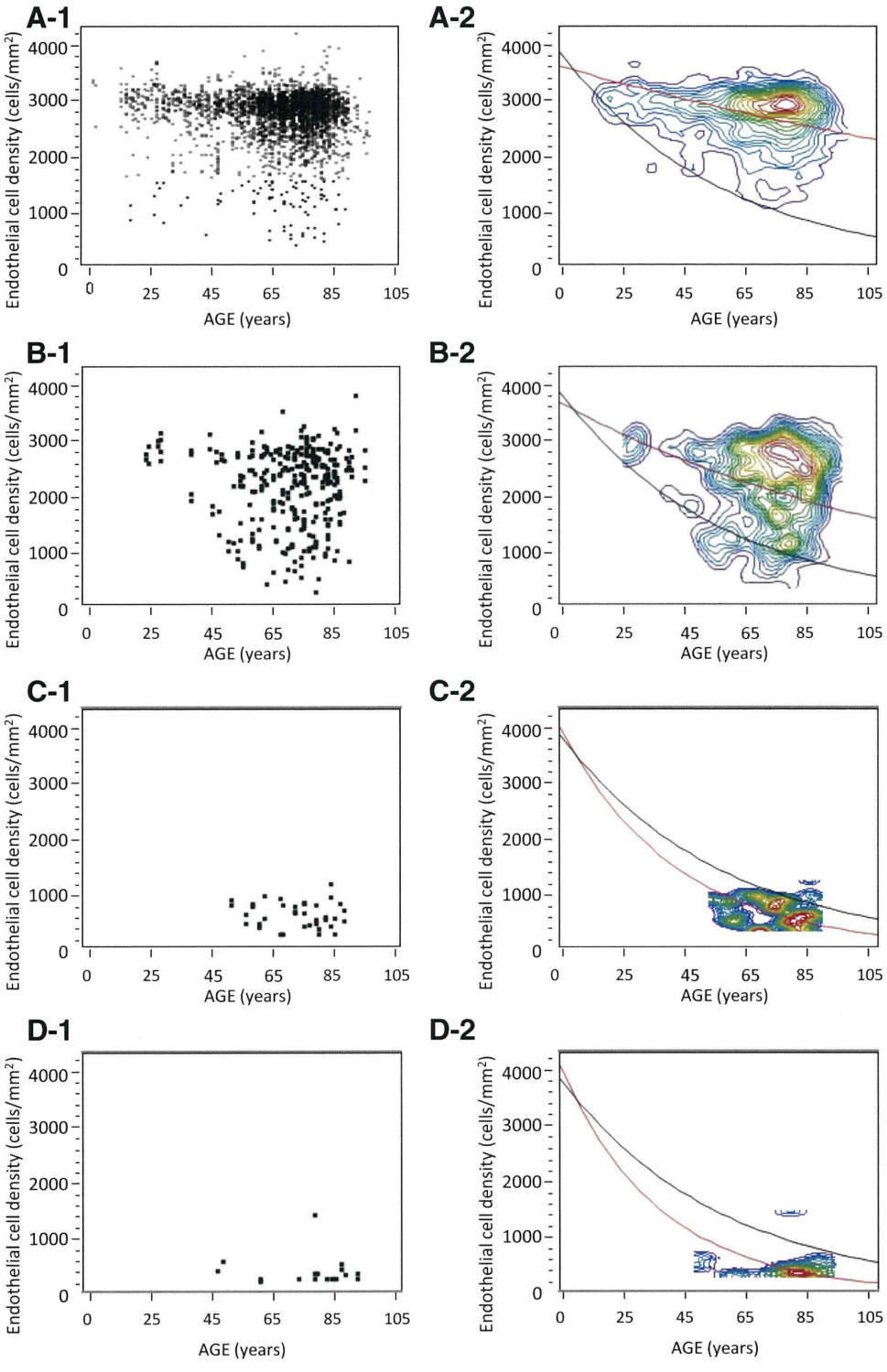

Figure 1. Scatterplots (*left*) and contour maps of nonparametric density smoothing (*right*) of each stage. (**A-1**, **A-2**) Stage 0, (**B-1**, **B-2**) stage 1, (**C-1**, **C-2**) stage 2, and (**D-1**, **D-2**) stage 3. *Red curves*: age-ECD curves of each stage calculated by least-squares method. The decrease rates of each stage were 0.44% (stage 0), 0.81% (stage 1), 2.65% (stage 2), and 3.08% (stage 3). The contour maps showed that the age-ECD curve of 2.00% decrease rate ($ECO_{2.0}$, *black curves*) ran through a trough between peaks of all stages. Most of the peaks in stages 0 and 1 were located above $ECO_{2.0}$, whereas peaks of stages 2 and 3 were located below $ECO_{2.0}$.

normal eyes reported in previous studies (Table 3).[10,12–16] Contour maps show that most of the peaks in stage 0 and 1 were located above the age-ECD curve of the 2.00% decrease rate, whereas peaks of stage 2 and 3 were located below this curve. Table 4 shows binary classification based on the age-ECD curve of a 2.00% decrease rate, designated novel ECD cutoff 2 ($ECO_{2.0}$), dividing stages 0+1 and stages 2+3 (Table 4) or stage 1 and stages 2+3 (Table 4). The high sensitivity and specificity of these classifications suggested that $ECO_{2.0}$ is an adequate cutoff between eyes with corneal edema and those without edema.

Age-ECD Curve of 1.4% and 2.0% Divides Stage 1 into Three Distinct Groups

The contour map of stage 1 consisted of several peaks. Figure 2 shows that the age-ECD curve of the 1.40% decrease rate, designated novel ECD-cutoff point 1 ($ECO_{1.4}$), divides these peaks into a high-density group ($>ECO_{1.4}$), and a low-density group ($<ECO_{1.4}$). ANOVA revealed that the age-ECD curves of each group predicted ECD according to age, with statistical significance: The F ratio and P value were 803.3 and <0.0001

TABLE 2. Mean ECD with Sample Sizes at 5-Year Intervals for Grades 0 to 3

	0–9 y		10–14 y		15–19 y		20–24 y		25–29 y	
	Eyes	**ECD**	**Eyes**	**ECD**	**Eyes**	**ECD**	**Eyes**	**ECD**	**Eyes**	**ECD**
Stage 0	4	3073.3 ± 392.6	7	3020.4 ± 330.1	47	2769.2 ± 530.1	31	2837.4 ± 567.3	60	2853.1 ± 507.6
Stage 1	0	—	0	—	0	—	4	2765.0 ± 128.8	6	2954.5 ± 175.6
Stage 2	0	—	0	—	0	—	0	—	0	—
Stage 3	0	—	0	—	0	—	0	—	0	—
	30–34 y		**35–39 y**		**40–44 y**		**45–49 y**		**50–54 y**	
	Eyes	**ECD**	**Eyes**	**ECD**	**Eyes**	**ECD**	**Eyes**	**ECD**	**Eyes**	**ECD**
Stage 0	58	2732.6 ± 511.3	54	2741.9 ± 324.7	80	2672.2 ± 462.5	99	2687.8 ± 507.8	128	2754.6 ± 370.5
Stage 1	0	—	4	2423.0 ± 474.1	7	2503.7 ± 541.9	7	1934.3 ± 763.9	14	1865.2 ± 703.0
Stage 2	0	—	0	—	0	—	2	881.0 ± 60.8	2	592.0 ± 120.2
Stage 3	0	—	0	—	1	461.0	1	622.0	0	—
	55–59 y		**60–64 y**		**65–69 y**		**70–74 y**		**75–79 y**	
	Eyes	**ECD**	**Eyes**	**ECD**	**Eyes**	**ECD**	**Eyes**	**ECD**	**Eyes**	**ECD**
Stage 0	195	2701.2 ± 408.1	325	2671.9 ± 464.4	384	2677.7 ± 449.1	494	2698.4 ± 435.0	496	2691.2 ± 421.3
Stage 1	25	2105.2 ± 673.3	28	2219.4 ± 695.5	39	2124.8 ± 743.7	61	2242.5 ± 719.4	44	2159.0 ± 741.7
Stage 2	4	645.8 ± 224.3	2	797.5 ± 282.1	7	562.9 ± 329.5	7	730.7 ± 149.5	7	483.0 ± 183.7
Stage 3	2	284.5 ± 21.9	0	—	0	—	2	302.5 ± 3.5	7	524.0 ± 418.9
	80–84 y		**85–89 y**		**≥90 y**					
	Eyes	**ECD**	**Eyes**	**ECD**	**Eyes**	**ECD**				
Stage 0	309	2698.9 ± 440.4	116	2624.5 ± 457.3	22	2563.7 ± 299.3				
Stage 1	47	2264.2 ± 556.2	17	2279.2 ± 597.9	5	2962.0 ± 597.1				
Stage 2	7	680.6 ± 318.1	3	723.3 ± 155.7	0	—				
Stage 3	5	302.4 ± 5.4	3	482.3 ± 97.1	2	352.5 ± 74.2				

Eye data are expressed as the number, and the ECD in cells per square millimeter.

in the high-density group and 945.7 and <0.0001 in the low-density group. The decrease rate of the age-ECD curve in the high-density group was 0.56%, which was very close to that of the stage 0 age-ECD curve. On the other hand, the decrease rate in the low-density group was 2.00%, which coincided with $ECO_{2.0}$. These results suggest that the decrease rate of the high-density group in stage 1 was nearly normal, whereas the low-density group in stage 1 was located on the border between eyes with and without corneal edema. We therefore classified stage 1 on the basis of $ECO_{1.4}$ and $ECO_{2.0}$, as follows (Fig. 3):

Stage 1a, asymptomatic guttata cornea (AGC): above $ECO_{1.4}$

Stage 1b, borderline guttata cornea (BGC): between $ECO_{1.4}$ and $ECO_{2.0}$

Stage 1c, preliminary stage of FCD (pre-FCD): below $ECO_{2.0}$

TABLE 3. Decrease Rates of Stage 0 in the Present Study and Normal Unoperated Eyes Reported in the Previous Studies

Author	Decrease Rate (%/y)	Nation
Murphy et al.[10]	0.56	United States
Cheng et al.[12]	1.00	England
Ambrose et al.[13]	0.60	England
Numa et al.[14]	0.30	Japan
Bourne et al.[15]	0.60	United States
Rao et al.[16]	0.30	India
Present study	0.44	Japan

DISCUSSION

To obtain a sufficient number of age-ECD data to compare FCD (stage 2+3), guttata cornea without edema (stage 1), and control group without guttata cornea (stage 0), we performed a retro-

TABLE 4. Binary Classification of Clinical Stage

Clinical Stage	Classification Based On $ECO_{2.0}$		
	Below $ECO_{2.0}$	**Above $ECO_{2.0}$**	**Total**
Total Eyes			
Stage 2+3	60	4	64
Stage 0+1	122	3095	3217
Total	182	3099	3281
Sensitivity, %	93.75		
Specificity, %	96.21		
Eyes with Guttata Cornea			
Stage 2+3	60	4	64
Stage 1	27	281	308
Total	87	285	372
Sensitivity, %	93.75		
Specificity, %	91.23		

Data are based on the age-ECD curve of 2.00% decrease rate as a novel ECD-cut-off ($ECO_{2.0}$), sensitivity and specificity to detect stage 2+3 from total eyes or the eyes with guttata cornea based on the classification.

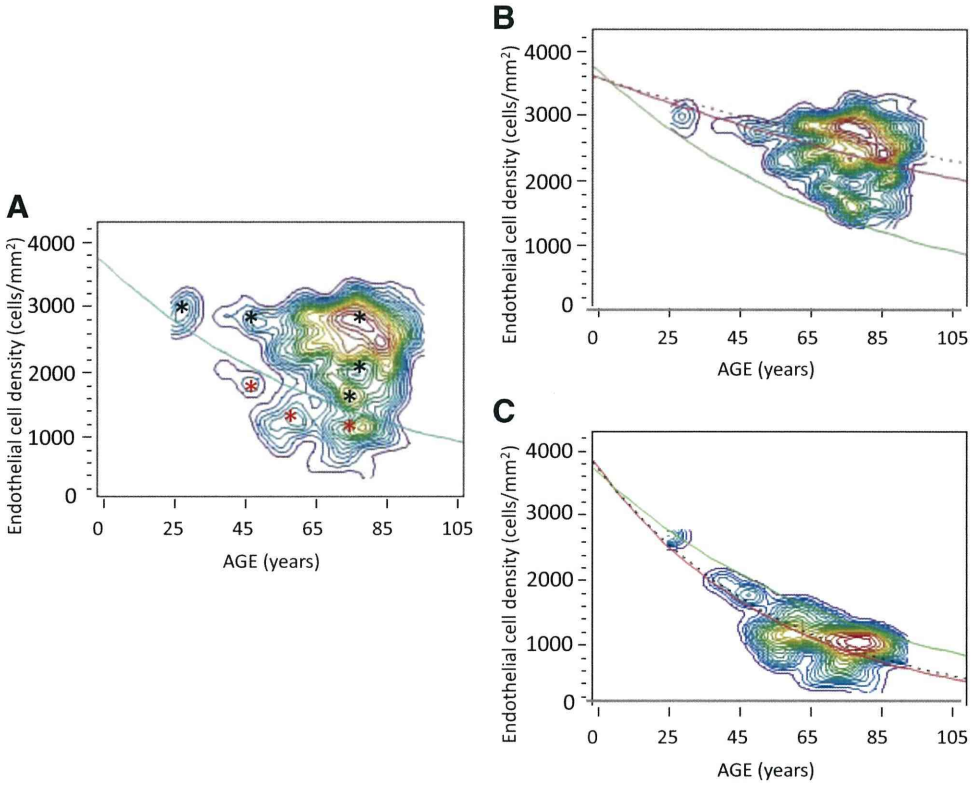

Figure 2. (**A**) The contour map of nonparametric density smoothing in stage 1. Stage 1 consisted of several peaks, and the age-ECD curve of 1.40% decrease rate ($ECO_{1.4}$, *green curve*) ran through a trough between peaks of high ECD group (*black asterisks*) and low ECD group (*red asterisks*). (**B**) High-density group in stage 1 above $ECO_{1.4}$. The age-ECD curve of this group (*red curve*) was close to that of stage 0 (*red dotted curve*), and the calculated decrease rate was 0.56%. (**C**) Low-density group in stage 1 below $ECO_{1.4}$. The age-ECD curve of this group (*red curve*) coincided with $ECO_{2.0}$ (*black dotted curve*), with a decrease rate of 2.00%.

spective, hospital-based review of total 1971 outpatients. In this study, we found a somewhat higher prevalence of guttata cornea than that found in previous reports in Japan. The prevalence of corneal guttae was reported to be 3.7% (1.5% in men, 5.5% in women) in Japan,[17,18] whereas it ranges from approximately 7% up to a remarkable 70.4% in North America, Iceland, and Europe.[1,8,19] In our study, the fact that subjects were hospital-based may have caused a higher prevalence. However, such bias does not have an effect on the validity of the mathematical model derived from the data. The following tendency of prevalence was apparent in our group of subjects: First, females were more predisposed to stages 1, 2, and 3 than were males, and the female ratio increased as stages progressed. Second, the prevalence of FCD was much smaller than stage 1. An increase in the female ratio in progressing stages suggested that sex may have some role not only in the onset but also the progression of the disease. Apparent difference of prevalence between FCD and stage 1 suggest the existence of a patient group in stage 1 that does not progress to corneal edema despite having guttata cornea.

Our model is based on the assumptions that the ECD at 5 years of age is common to all classes and that the decrease rate

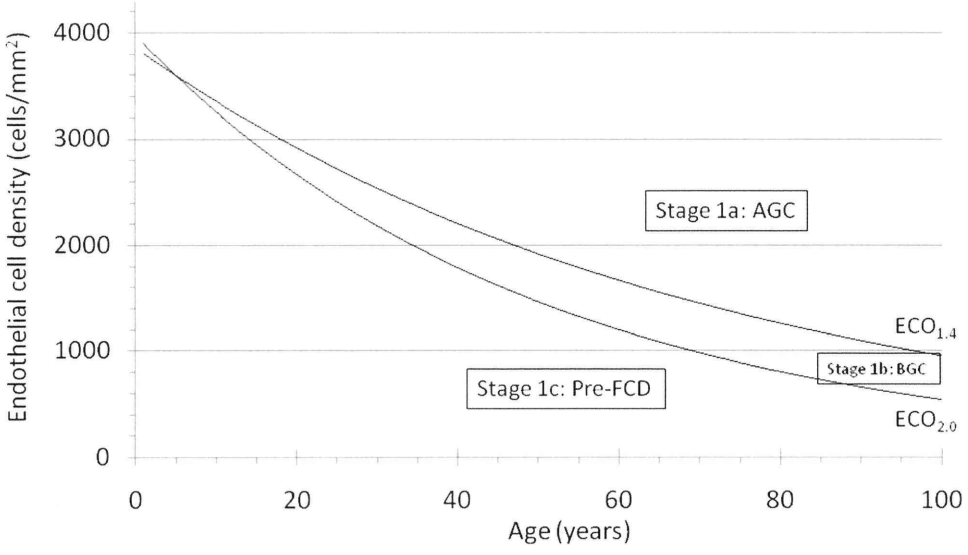

Age (years)		20	30	40	50	60	70	80	90
ECD (cells/mm²)	ECO_{14}	2918	2537	2205	1917	1667	1449	1260	1095
	ECO_{20}	2667	2184	1788	1464	1198	981	803	658

Figure 3. Proposed classification of eyes in stage 1 based on $ECO_{1.4}$ and $ECO_{2.0}$. Eyes in stage 1a above $ECO_{1.4}$ were named AGC, which had a decrease rate as low as stage 0. Eyes in stage 1c below $ECO_{2.0}$ had a decrease rate as high as FCD (stages 2 and 3), and therefore, this stage was named pre-FCD. Stage 1b between $ECO_{1.4}$ and $ECO_{2.0}$ was named BGC. The table below the graph shows the coordinates of $ECO_{1.4}$ and $ECO_{2.0}$.

of ECD percentage per year) is constant but with a different value of each class. The use of these assumptions may be a debatable point when discussing the validity of our study. However, the results of our mathematical model show ECD decrease rates that are acceptable when compared with clinical observations. The decrease rate of 0.44% in stage 0 is within the range of values of normal unoperated eyes reported in the previous studies.[10,12–16] Furthermore, since $ECO_{1.4}$ and $ECO_{2.0}$ runs through a clearly defined trough between peaks on the scatterplot, and $ECO_{2.0}$ divided stages 0+1 and stages 2+3 or stage 1 and stages 2+3 with high sensitivity and specificity, we believe our mathematical model for classifying patients with guttae based on ECD decrease rates is adequate for predicting the prognosis.

The $ECO_{1.4}$ and $ECO_{2.0}$ curves based on our mathematical model divided stage 1 into three subgroups, stage 1a, 1b, and 1c. The ECD decrease rate of stage 1a was close to that of stage 0, that is, almost normal. Schnitzer and Krachmer reported on 44 relatives of 12 families with guttata cornea which appeared normal on slit-lamp examination and endothelial cell parameters.[20] These eyes presumably belonged to stage 1a of our classification. In addition, because the distribution of patients of stage 1a was located above $ECO_{1.4}$, the risk of progressing to corneal edema may be as low as stage 0. If a patient was on the curve of a 1.4% decrease rate, the ECD would be 1095 cells/mm^2 even when he was 90 years old. Presumption of low risk of stage 1 is supported by analysis of variance, showing that age-ECD curves of each stage had significant predictability.

It was surprising that the age-ECD curve of the low-density group of stage 1 (stages 1b and 1c) coincided completely with $ECO_{2.0}$. The former was calculated by the least-squares method of the low-density group of stage 1, whereas the latter was obtained from trough between peaks of stages 0 to 3 on scatterplots. This result suggests that the low-density group of stage 1 was located on the border between stage 0 and FCD. Eyes in stage 1c below $ECO_{2.0}$ have a decrease rate as high as FCD, suggesting that these eyes have a risk to progress to FCD, even if there was no corneal edema present. This was the rationale for referring to stage 1c as pre-FCD. Further prospective study of patients in stage 1b and 1c is needed to determine whether stage 1c is a preliminary stage of FCD.

Recently, several pathogenic mechanisms, such as oxidative stress or unfolded protein response, have been reported as causes of FCD.[21,22] The difference in resistance against such stress may cause the difference in decrease rates between stages. Previous reports suggested that ECD of some eyes with guttata cornea did not decrease significantly compared with normal eyes after cataract surgery,[7,23] whereas some eyes in other reports showed a significantly higher decrease.[24] When we adapted data from these reports to our classification, we found that most of the former eyes with no difference in ECD (18/21 eyes) were categorized as stage 1a, suggesting that our classification may be used to identify patients with a higher risk of endothelial damage due to external stress. Future studies on guttata corneas using our classification may help clarify the mechanism of FCD progression.

In conclusion, we assessed distribution and endothelial loss rate of guttata cornea stages 0 to 3 and determined new cutoff curves $ECO_{1.4}$ and $ECO_{2.0}$ by using scatterplots. Our mathematical model is a simple method for predicting the prognosis of patients with guttata cornea.

References

1. Weisenthal RW, Streeten BW, eds. *Posterior Membrane Dystrophies.* London: Elsevier Mosby; 2005.
2. Edelhauser HF, Ubels JL, eds. *The Cornea and the Sclera.* 10th ed. ed. St. Louis: Mosby; 2003.
3. Al-Yousuf N, Mavrikakis I, Mavrikakis E, Daya SM. Penetrating keratoplasty: indications over a 10 year period. *Br J Ophthalmol.* 2004;88(8):998–1001.
4. Dobbins KR, Price FW Jr, Whitson WE. Trends in the indications for penetrating keratoplasty in the midwestern United States. *Cornea.* 2000;19(6):813–816.
5. Kang PC, Klintworth GK, Kim T, et al. Trends in the indications for penetrating keratoplasty. 1980–2001. *Cornea.* 2005;24(7):801–803.
6. Krachmer JH, Purcell JJ Jr, Young CW, Bucher KD. Corneal endothelial dystrophy: a study of 64 families. *Arch Ophthalmol.* 1978; 96(11):2036–2039.
7. Kitagawa K, Fujisawa A, Mizuno T, Sasaki K. Twenty-three cases of primary cornea guttata. *Jpn J Ophthalmol.* 2001;45(1):93–98.
8. Adamis AP, Filatov V, Tripathi BJ, Tripathi RC. Fuchs' endothelial dystrophy of the cornea. *Surv Ophthalmol.* 1993;38(2):149–168.
9. Stocker FW. The endothelium of the cornea and its clinical implications. *Trans Am Ophthalmol Soc.* 1953;51:669–786.
10. Murphy C, Alvarado J, Juster R, Maglio M. Prenatal and postnatal cellularity of the human corneal endothelium: a quantitative histologic study. *Invest Ophthalmol Vis Sci.* 1984;25(3):312–322.
11. Nucci P, Brancato R, Mets MB, Shevell SK. Normal endothelial cell density range in childhood. *Arch Ophthalmol.* 1990;108(2):247–248.
12. Cheng H, Jacobs PM, McPherson K, Noble MJ. Precision of cell density estimates and endothelial cell loss with age. *Arch Ophthalmol.* 1985;103(10):1478–1481.
13. Ambrose VM, Walters RF, Batterbury M, Spalton DJ, McGill JI. Long-term endothelial cell loss and breakdown of the blood-aqueous barrier in cataract surgery. *J Cataract Refract Surg.* 1991; 17(5):622–627.
14. Numa A, Nakamura J, Takashima M, Kani K. Long-term corneal endothelial changes after intraocular lens implantation: anterior vs posterior chamber lenses. *Jpn J Ophthalmol.* 1993;37(1):78–87.
15. Bourne WM, Nelson LR, Hodge DO. Central corneal endothelial cell changes over a ten-year period. *Invest Ophthalmol Vis Sci.* 1997;38(3):779–782.
16. Rao SK, Ranjan Sen P, Fogla R, Gangadharan S, Padmanabhan P, Badrinath SS. Corneal endothelial cell density and morphology in normal Indian eyes. *Cornea.* 2000;19(6):820–823.
17. Kitagawa K, Kojima M, Sasaki H, et al. Prevalence of primary cornea guttata and morphology of corneal endothelium in aging Japanese and Singaporean subjects. *Ophthalmic Res.* 2002;34(3): 135–138.
18. Nagaki Y, Hayasaka S, Kitagawa K, Yamamoto S. Primary cornea guttata in Japanese patients with cataract: specular microscopic observations. *Jpn J Ophthalmol.* 1996;40(4):520–525.
19. Zoega GM, Fujisawa A, Sasaki H, et al. Prevalence and risk factors for cornea guttata in the Reykjavik Eye Study. *Ophthalmology.* 2006 Apr;113(4):565–569.
20. Schnitzer JI, Krachmer JH. A specular microscopic study of families with endothelial dystrophy. *Br J Ophthalmol.* 1981;65(6): 396–400.
21. Buddi R, Lin B, Atilano SR, Zorapapel NC, Kenney MC, Brown DJ. Evidence of oxidative stress in human corneal diseases. *J Histochem Cytochem.* 2002;50(3):341–351.
22. Engler C, Kelliher C, Spitze AR, Speck CL, Eberhart CG, Jun AS. Unfolded protein response in Fuchs endothelial corneal dystrophy: a unifying pathogenic pathway? *Am J Ophthalmol.* 2010;149(2):194–202-e2.
23. Stur M, Grabner G, Dorda W. Changes of the corneal endothelium following intracapsular cataract extraction with implantation of semiflexible anterior chamber lenses. I. Results of the early postoperative period. *Acta Ophthalmol (Copenh).* 1984;62(4):586–594.
24. Bourne WM, Nelson LR, Hodge DO. Continued endothelial cell loss ten years after lens implantation. *Ophthalmology.* 1994; 101(6):1014–1022.

Clinical Significance of Owl Eye Morphologic Features by In Vivo Laser Confocal Microscopy in Patients with Cytomegalovirus Corneal Endotheliitis

AKIRA KOBAYASHI, HIDEAKI YOKOGAWA, TOMOMI HIGASHIDE, KOJI NITTA, AND KAZUHISA SUGIYAMA

• OBJECTIVE: To demonstrate the clinical significance of owl eye morphologic features observed by in vivo laser confocal microscopy in patients with cytomegalovirus (CMV) corneal endotheliitis.

• DESIGN: Observational case series.

• METHODS: PARTICIPANTS: Six eyes of 6 patients (6 men; mean age, 73.3 years) with cytomegalovirus corneal endotheliitis diagnosed by clinical manifestations together with polymerase chain reaction from aqueous humor samples. INTERVENTION: All patients were examined by slit-lamp biomicroscopy and in vivo laser confocal microscopy. MAIN OUTCOME MEASURES: Clinical manifestations were summarized by reviewing medical records. Selected confocal images of corneal layers were evaluated qualitatively for shape and degree of light reflection of abnormal cells and deposits.

• RESULTS: All patients had long histories of anterior uveitis with intraocular pressure elevation, corneal edema with keratic precipitates, and decrease of endothelial cell densities. Coin-shaped lesions were observed by slit lamp only in 1 patient at the first visit and in 2 additional patients at subsequent follow-up. In all patients, confocal microscopy demonstrated reduced subepithelial nerves, subepithelial opacity, increased reflectivity of keratocytes, highly reflective dots, and needle-shaped bodies. Owl eye morphologic features were observed consistently in all patients at the initial visit, and highly reflective round bodies were detected in 5 patients; most notably, these confocal features were reversible after resolution of endotheliitis.

• CONCLUSIONS: Owl eye morphologic features and highly reflective round bodies observed by confocal microscopy may be useful as an adjunct for the noninvasive diagnosis of cytomegalovirus corneal endotheliitis. Reversibility of these features after resolution of endotheliitis may be useful for monitoring the therapeutic effects without multiple anterior chamber tap. (Am J Ophthalmol 2011; xx:xxx. © 2011 by Elsevier Inc. All rights reserved.)

Accepted for publication July 28, 2011.

From the Department of Ophthalmology, Kanazawa University Graduate School of Medical Science, Kanazawa, Japan (A.K., H.Y., T.H., K.S.); and the Department of Ophthalmology, Fukui-ken Saiseikai Hospital, Fukui, Japan (K.N.).

Inquiries to Akira Kobayashi, Department of Ophthalmology, Kanazawa University Graduate School of Medical Science, 13-1 Takara-machi, Kanazawa-shi, Ishikawa-ken 920-8641 Japan; e-mail: kobaya@kenroku.kanazawa-u.ac.jp

CORNEAL ENDOTHELIITIS, CHARACTERIZED BY CORneal edema associated with linear keratic precipitates and endothelial dysfunction,[1] may be caused by herpes simplex virus (HSV),[2] varicella zoster virus (VZV),[3] or other viruses such as mumps.[4] It often leads to irreversible corneal endothelial cell damage and severe visual disturbance. Most recently, cytomegalovirus (CMV) was recognized as a new etiologic factor for corneal endotheliitis.[5] Clinical manifestations of CMV endotheliitis are characterized by linear keratic precipitates associated with multiple coin-shaped lesions and local corneal stromal edema with minimal anterior chamber reactions.[6] The intraocular pressure (IOP) of these patients frequently is increased, and they often are treated with topical or systemic antiglaucoma medication because of the diagnosis of secondary glaucoma of unknown origin.[6] The patients also may have had past histories of several penetrating keratoplasties.[6–8]

In vivo white-light confocal microscopy has been used as a noninvasive technique for the observation of normal and pathologic corneal microstructures at the cellular level in real time.[9–13] Most recently, new-generation scanning laser in vivo confocal microscopy (Heidelberg Retina Tomograph 2 Rostock Cornea Module [HRT 2-RCM]; Heidelberg Engineering GmbH, Dossenheim, Germany) has become available.[14–16] This new device provides high-definition histologic-like images of corneal microstructures in vivo, with an axial resolution of approximately 4 μm and improved resolution compared with conventional white-light confocal microscopes (for example, 10 μm axial optical resolution with ConfoScan 2 [Nidek Technologies, Vigonza, Italy]).[17,18] Previously, Shiraishi and associates demonstrated large corneal endothelial cells with an area of high reflection in the nucleus surrounded by a halo of low reflection in a single patient with CMV corneal endotheliitis using the HRT 2-RCM.[19] The authors suggest that these owl eye morphologic features in the corneal endothelium may be characteristic of CMV endotheliitis. A small number of case reports also have suggested an association of owl eye morphologic features in the corneal endothelium and CMV corneal endotheliitis.[6,8]

In this article, we report clinical manifestations in 6 Japanese patients with polymerase chain reaction (PCR)-proven CMV corneal endotheliitis and the re-

0002-9394/$36.00
doi:10.1016/j.ajo.2011.07.026

TABLE. Clinical Data and Slit-Lamp Biomicroscopic Findings of 6 Patients with Cytomegalovirus Corneal Endotheliitis

Case No.	Gender/ Age (y)	Age (y)	Affected Eye	History of Ocular Disease and Duration (mos)	Slit-Lamp Findings	Endothelial Cell Density (cells/mm^2)
1	M	77	Left	Anterior uveitis, secondary glaucoma (72)	Corneal edema, pigmented KPs (coin-shaped lesions during follow-up), AC cell	692
2	M	75	Left	Anterior uveitis, secondary glaucoma (24), diagnosed as Posner- Schlossman syndrome	Corneal edema, pigmented KPs, coin-shaped lesions, AC cell	1730
3	M	63	Right	Anterior uveitis, secondary glaucoma (108), diagnosed as Posner-Schlossman syndrome	Corneal edema, pigmented KPs (coin-shaped lesions during follow-up), AC cell+, iris atrophy	1677
4	M	83	Right	Anterior uveitis, secondary glaucoma (60)	Corneal edema, Pigmented KPs AC cell+, fibrin+	645
5	M	56	Left	Anterior uveitis, secondary glaucoma, (144), diagnosed as Posner-Schlossman syndrome	Corneal edema, pigmented KPs, AC cell+, iris atrophy	<1000
6	M	86	Left	Anterior uveitis, secondary glaucoma (96), diagnosed as Posner- Schlossman syndrome	Corneal edema, pigmented KPs, AC cell, depigmented iris	550

AC = anterior chamber; CMV = cytomegalovirus; DNA = deoxyribonucleic acid; DM = diabetes mellitus; Dx = diamox; F = female; KPs = keratic precipitates; M = male; PCR = polymerase chain reaction. *Continued on next page*

sults of detailed investigations of in vivo corneal microstructures of all cell layers with laser scanning confocal microscopy using the HRT 2-RCM. The diagnostic value and usefulness of monitoring the therapeutic effects of this device in CMV corneal endotheliitis also are described.

METHODS

THE STUDY POPULATION CONSISTED OF 6 EYES OF 6 CONsecutive patients (6 men; mean, 73.3 years), whose active CMV corneal endotheliitis was diagnosed and treated between April 2010 and March 2011 at the Department of Ophthalmology, Kanazawa University Hospital, Kanazawa, Japan (Patients 1 through 5), or the Department of Ophthalmology, Fukui-ken Saiseikai Hospital, Fukui, Japan (Patient 6; Table). The clinical diagnosis was performed based on slit-lamp findings of active corneal endotheliitis (such as corneal edema and keratic precipitates) and the detection of CMV by PCR assay in the aqueous humor from the affected eye. HSV, VZV, Epstein-Barr virus, human herpes virus 6, and human herpes virus 7 DNA were not detected. Clinical manifestations of the patients were reviewed retrospectively, with special attention paid to slit-lamp findings, IOP measurements, and corneal endothelial cell density. Also, responses to antiviral treatment were evaluated.

• IN VIVO LASER CONFOCAL MICROSCOPY: Before examination, written informed consent was obtained from all subjects after explaining the nature and possible consequences of this study, such as superficial punctate keratopathy. After applying a large drop of contact gel (Comfort Gel ophthalmic ointment; Bausch & Lomb GmbH, Berlin, Germany) on the front surface of the microscope lens and ensuring that no air bubbles had formed, a Tomo-Cap (Heidelberg Engineering GmbH, Dossenheim, Germany) was mounted on the holder to cover the microscope lens. The central and affected areas of the cornea then were examined layer by layer using the HRT 2-RCM. The HRT 2-RCM uses a ×60 water-immersion objective lens (Olympus Europa GmbH, Hamburg, Germany) and uses a 670-nm diode laser as the light source with a 400-μm^2 area of observation.

RESULTS

• CLINICAL MANIFESTATIONS: The Table summarizes the clinical manifestations for 6 eyes of 6 patients. The mean follow-up period for all patients was 4.2 ± 2.5

TABLE. Clinical Data and Slit-Lamp Biomicroscopic Findings of 6 Patients with Cytomegalovirus Corneal Endotheliitis *(Continued)*

Systemic Disease	Intraocular Pressure (mm Hg) (No. Antiglaucoma Eye Drops)	Visual Acuity before/after Treatment	CMV DNA by PCR of Aqueous Humor	Treatment	Clinical Outcomes (Follow-up Period after CMV Detection, mos)
DM, mixed connective tissue disease (oral prednisolone 2.5 mg/day)	18 (1)	20/25/20/25	Positive	Systemic ganciclovir 10 mg/kg daily × 7 days, 0.5% ganciclovir, 8 times daily, 0.1% betamethasone, 4 times daily	Clear cornea (8)
Lung cancer (treated)	25 (3+Dx)	20/40/20/40	Positive	0.5% ganciclovir 8 times daily, 0.1% betamethasone 4 times daily	Clear cornea (5)
Hyperlipidemia, fatty liver	24 (3+Dx)	20/25/20/25	Positive	Systemic ganciclovir 10 mg/kg daily × 7 days, 0.5% ganciclovir 8 times daily, 0.1% betamethasone 4 times daily, cataract surgery for secondary cataract	Edema reduction (5)
Essential thrombocythemia	26 (2)	20/100/20/40	Positive	0.5% ganciclovir 8 times daily, 0.1% betamethasone 4 times daily	Clear cornea (4)
DM	15 (4)	20/100/12/40	Positive	Systemic ganciclovir 1800 mg daily × 12 days, 0.5% ganciclovir 8 times daily, 0.1% betamethasone 4 times daily	Edema reduction (2)
Hypertension	43 (3+Dx)	20/22/20/16	Positive	Systemic ganciclovir 10 mg/kg daily × 14 days, 0.5% ganciclovir 8 times daily, 0.1% betamethasone 4 times daily	Edema reduction (1)

months (range, 1 to 8 months). All patients were male (6/6; 100%) and had long histories (more than 2 years) of anterior uveitis (6/6; 100%) and IOP elevation of unknown origin (6/6; 100%) that was treated by corticosteroids and antiglaucoma agents (duration, 24 to 144 months; mean ± standard deviation, 84.0 ± 41.6 months). All patients had corneal edema (6/6; 100%) and pigmented keratic precipitates (6/6; 100%). Three patients had mild anterior chamber reaction (Patients 3 through 5; 50%), and the remaining 3 patients had no anterior chamber reaction. Iris atrophy was observed in 3 patients (Patients 3, 5, and 6; 3/6; 50%). Three patients experienced strong iridocyclitis with fibrin reaction after cataract surgery (3/4; 75%); the surgery was performed before the diagnosis of CMV endotheliitis in 1 patient and after the treatment of CMV endotheliitis in 2 patients. A tentative diagnosis of Posner-Schlossman syndrome was made in 4 patients (Patients 2, 3, 5, and 6; 4/6; 66.7%), and 5 patients (5/6, 83.3%) initially were referred to our glaucoma service. Severe glaucomatous visual field defects were observed in 2 patients (2/6; 33.3%).

Coin-shaped lesions were observed only in Patient 2 at the first visit. At subsequent follow-up visits, 2 additional patients had coin-shaped lesions (Patients 1 and 3; total, 3/6; 50%: Figure 1). The coin-shaped lesions were not detectable in the remaining 3 patients (Patients 4 through 6) throughout the follow-up period. Endothelial cell density (ECD) was decreased in all eyes (6/6; 100%); 4 patients (Patients 1, 4, 5, and 6) had an ECD of less than 1000/mm^2, and the remaining 2 patients had an ECD of less than 2000/mm^2. Patients 1 and 5 had diabetes mellitus, and Patient 1 also had mixed connective tissue disease treated with oral prednisolone 2.5 mg/day. The aqueous humor samples of all eyes contained CMV DNA (6/6; 100%), but not HSV, VZV, Epstein-Barr virus, human herpes virus 6, or human herpes virus 7 DNA. All patients were treated with topical 0.5% ganciclovir (8 times daily) and 0.1% betamethasone (4 times daily). In addition, all patients (except Patients 2 and 4) were administrated intravenous ganciclovir 10 mg/kg daily for 7 days based on the severity of clinical manifestations. After 1 to 2 months of treatment, corneal edema, keratic precipitates (KPs), and IOP were improved in all patients. In Patients 1 and 3, CMV DNA was not detected by PCR in aqueous humor samples after treatment. CMV DNA was not tested again in the remaining patients.

• IN VIVO LASER CONFOCAL MICROSCOPY: In vivo laser confocal microscopy demonstrated normal epithelial layers in 4 patients (Patients 1, 2, 4, and 5; 66.7%) and slightly increased cell body size with higher intensity indicative of epithelial edema in 2 patients (Patients 3 and 6; 33.3%: Figure 2, Top right). A few subepithelial nerves were detected in 2 patients (Patients 3 and 4; 33.3%; Figure 2,

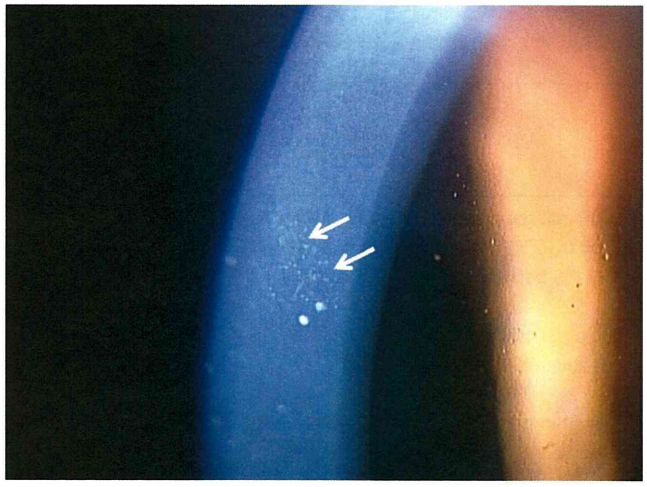

FIGURE 1. Coin-shaped lesion identified by slit lamp in a patient with cytomegalovirus corneal endotheliitis. Coin-shaped lesion was observed in Patient 1 during the follow-up period (arrows). This was not noted at the initial visit.

Second row left), but no subepithelial nerves were detected in the remaining 4 patients (Patients 1, 2, 5, and 6; 66.7%; Figure 3, Second row left; Figure 4, Second row left). Stromal nerves were detected in 2 patients (Patients 2 and 3; 33.3%). Subepithelial opacity, increased reflectivity of keratocytes, highly reflective dots, and needle-shaped bodies were observed uniformly in all patients (6/6; 100%; Figure 3, Second row center and Second row right; Figure 4, Second row center and Second row right; Figure 2, Second row center and Second row right). The most characteristic feature was large cells whose nuclei had a high reflection area surrounded by a halo of low reflection (owl eye morphologic features), and these were observed in the corneal endothelial cell layer in all eyes (6/6; 100%; Figure 2, Bottom left and Bottom center, Figure 3, Third row left, Third row center, Third row right, and Bottom center; Figure 4, Bottom left and Bottom center). In contrast, owl eye morphologic features were not detected by noncontact specular microscopy in any of the patients (data not shown). Highly reflective round bodies on the surface of the endothelial cell layer also were detectable in 5 patients (Patients 1 through 3, 5, and 6; 83.3%; Figure 2, Bottom right, Figure 3, Bottom left, Bottom center, Bottom right; Figure 4, Bottom right). These owl eye cells and highly reflective round bodies disappeared in all patients after treatment. Subepithelial and stromal nerves were visible in all patients after resolution of the CMV endotheliitis.

• CASE REPORT: A 75-year-old man (Case 2) began to experience recurrent episodes of anterior uveitis of unknown origin and IOP elevation to 40 mm Hg in his left eye in June 2008. He was diagnosed with bilateral glaucoma and Posner-Schlossman syndrome and was treated with topical corticosteroids and antiglaucoma agents. He was referred to the glaucoma service at our hospital in June 2010 for poor IOP control. He had a history of lung cancer (treated). At the initial visit, his BCVA was 20/40 in the left eye. His left cornea had localized corneal edema, pigmented KPs in the lower cornea, and coin-shaped lesions with minimal anterior chamber reaction (Figure 4, Top left and Top center). Iris atrophy was not noted. ECD was 1730 cells/mm^2 in his left eye and 2785 cells/mm^2 in his right eye. IOP was 9 mm Hg (right) and 25 mm Hg (left) with antiglaucoma agents (topical latanoprost, dorzolamide, bunazosin, and oral acetazolamide). Bilateral glaucomatous optic neuropathy was observed, but CMV retinitis was not observed by fundus examination. Owl eye morphologic features were observed by HRT2-RCM examination in his left eye (Figure 4, Bottom left and Bottom center). PCR analysis of aqueous humor samples for the left eye detected CMV, but not HSV, VZV, Epstein-Barr virus, human herpes virus 6, or human herpes virus 7 DNA. In August 2010, based on the diagnosis of CMV corneal endotheliitis in the left eye, topical 0.5% ganciclovir was applied 8 times daily, and 0.1% betamethasone was applied 4 times daily, but he was not treated with systemic ganciclovir. The corneal edema disappeared rapidly, and the KPs and IOP improved gradually. In November 2010, the owl eye morphologic features had disappeared in the endothelial layer by HRT2-RCM examination. In January 2011, the left eye IOP was reduced to 11 mm Hg under a single antiglaucomatous agent (topical dorzolamide only).

DISCUSSION

HEREIN, WE REPORT THE CLINICAL MANIFESTATIONS TOgether with detailed in vivo laser confocal microscopic findings of all corneal cell layers in 6 Japanese patients with PCR-proven CMV corneal endotheliitis. To the best of the authors' knowledge, this is the largest series of confocal microscopic analyses of CMV corneal endotheliitis. The main highlight of the case series is the supportive diagnostic value of owl eye morphologic features by confocal microscopy. Most notably, we found that these confocal features are reversible after resolution of corneal endotheliitis.

In vivo laser confocal microscopy demonstrated epithelial edema in 2 patients (2/6; 33.3%), reduced or nondetectable subepithelial nerves in all patients (100%; 6/6), reduced stromal nerves in 2 patients (2/6; 33.3%), subepithelial opacity in all patients (6/6; 100%), increased reflectivity of keratocytes in all patients (6/6; 100%), and highly reflective dots and needle-shaped bodies in all patients (6/6; 100%). These confocal characteristics most likely were the result of common pathologic changes seen in edematous cornea caused by endothelial dysfunction, corneal stromal inflammation, or both.[16,20–23] However,

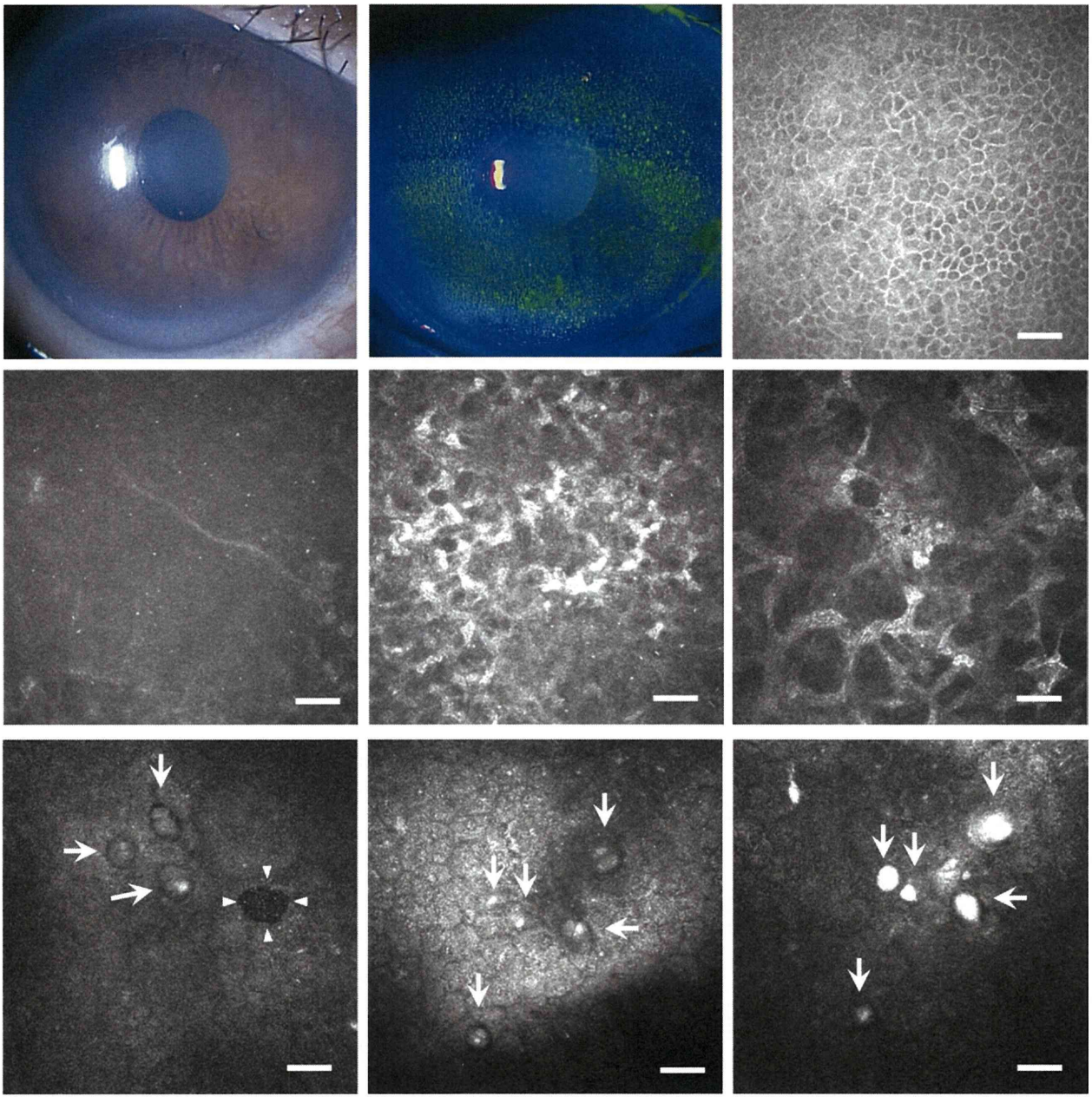

FIGURE 2. Slit-lamp photographs and laser confocal microscopy scans from a patient with cytomegalovirus corneal endotheliitis (Patient 3). (Top left) Slit-lamp photograph of the right cornea of Patient 3 at an initial visit to the hospital. Brown pigmented keratic precipitates were seen in the lower part of the cornea. (Top middle) Sectorial edemas from periphery to mid periphery were detected under fluorescein staining. (Top right) Epithelial basal cell layer in the center of the cornea showed slight edema by Heidelberg Retina Tomograph 2 Rostock Cornea Module (HRT 2-RCM). Bar = 50 μm. (Second row left) Bowman layer with highly reflective tiny dots. Nerve density was reduced. (Second row middle) Subepithelial opacity with increased reflectivity of keratocytes was observed. (Second row right) Highly reflective activated keratocytes were seen. (Bottom left and middle) Owl eye morphologic features were detectable by HRT 2-RCM (arrows). Endothelial cell density was 1677 cells/mm^2. (Bottom right) Sequential image of Bottom row middle, 8 μm forward toward the anterior chamber. Highly reflective round bodies, presumably the identical cell of owl eye morphologic features seen in Bottom row middle were noted (arrows).

the precise origin and significance of these pathologic changes remain unclear. It should be noted that subepithelial and stromal nerves were reversible in all cases after resolution of the CMV endotheliitis.

The most characteristic feature was large cells, whose nuclei had a high reflection area surrounded by a halo of low reflection (owl eye morphologic features), which were observed in the corneal endothelial cell layer by HRT2-

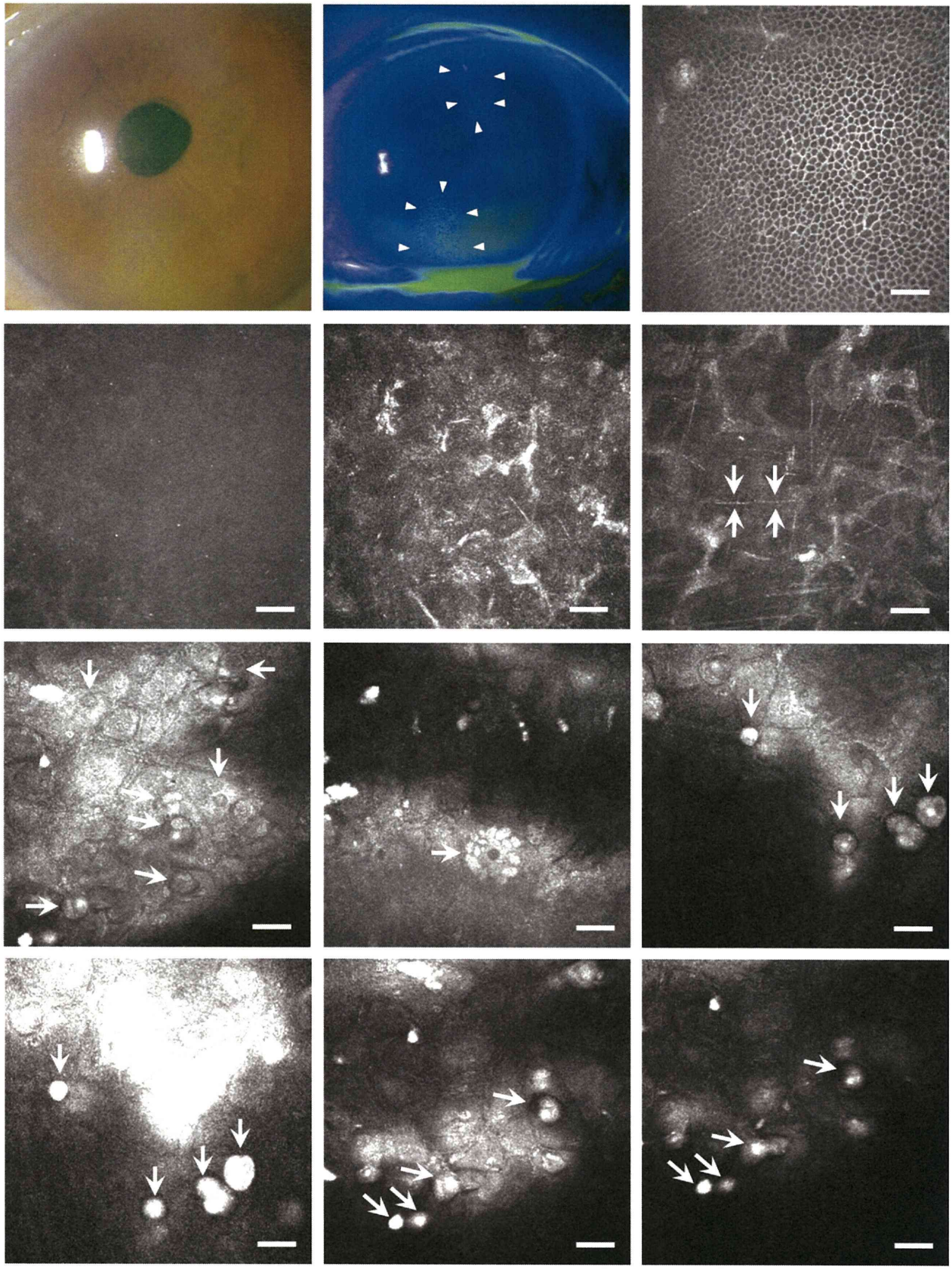

FIGURE 3. Slit-lamp photographs and laser confocal microscopy scans from a patient with cytomegalovirus corneal endotheliitis (Patient 1). (Top left and center) Slit-lamp photographs of the left cornea of Patient 1 at the initial visit to the hospital. Faint keratic

RCM in all eyes at the initial visit (6/6; 100%). This indicates the potential usefulness of visualizing owl eye morphologic features in the diagnosis of CMV corneal endotheliitis. Owl eye cells typically are seen at autopsy or in biopsy specimens from the kidneys, lungs, and other organs in cases of congenital or acquired CMV infection.[24] Shiraishi and associates were the first to report the owl eye morphologic features in a single case of CMV corneal endotheliitis using HRT2-RCM.[19] In their study, owl eye morphologic features in the corneal endothelial cell layer observed by in vivo laser confocal microscopy were described as "a group of large cells whose nuclei have a high reflection area surrounded by a halo of low reflection."[19] Subsequently, 2 case reports showed the presence of owl eye morphologic features by in vivo laser confocal microscopy in CMV corneal endotheliitis: Koizumi and associates reported an owl eye morphologic features in 1 patient, and Wang and associates reported 1 patient with owl eye morphologic features after penetrating keratoplasty.[6,8] In this study, we reported 6 cases of PCR-proven CMV corneal endotheliitis, and all cases (100%) demonstrated owl eye morphologic features by HRT2-RCM. Furthermore, the owl eye morphologic features disappeared after treatment in all patients. Thus, HRT2-RCM may be useful not only for diagnosing CMV corneal endotheliitis, but also for monitoring the therapeutic effects of systemic or topical antiviral drugs. Moreover, this may provide information regarding the timing for discontinuing medications in a noninvasive manner compared with PCR testing, which requires an anterior chamber tap. It should be noted that the owl eye morphologic features were not detected by noncontact specular microscopy in any of the patients. One explanation of this discrepancy of observation between the 2 diagnostic methods may be the difference of observational area. In specular microscopy, only the central endothelium is visualized. In contrast, by confocal microscopy, scanning a wide area of endothelium is possible, enabling rapid detection of owl eye morphologic features. Another important explanation is the difference of principals of visualizing the endothelium. In specular microscopy, specular reflection can be obtained only when the endothelium is smooth. Also, specular microscopy visualizes only the surface of the endothelial cells. In contrast, by confocal microscopy, all cell layers can be visualized with high resolution and pathologic endothelium, such as guttae seen in Fuchs dystrophy, can be observed clearly. Therefore, confocal microscopy may be a reasonable device to visualize the owl eye morphologic features, because the features are a characteristic light reflection inside the endothelial cells, which probably correspond to the intranuclear inclusion body.

One notable finding from our in vivo laser confocal microscopic study is that highly reflective round bodies with a diameter of 10 to 30 μm were observed on the surface of the corneal endothelium in 5 patients (5/6; 83.3%). These deposits did not look like the images of KPs usually seen in various kinds of uveitis.[25,26] On careful examination using consecutive images around the level of the endothelial cell layer, we noted that these deposits were localized on the surface of the endothelial cells and were related to the owl eye morphologic features (Figure 2, Bottom row middle and right, Figure 3, Third row right, Bottom row). We assumed that the highly reflective round bodies were CMV infected and were necrotic endothelial cells that protruded or had fallen off toward the anterior chamber. The fact that highly reflective round bodies disappeared after treatment in all patients also suggests that these are closely related to the owl eye morphologic features.

Koizumi and associates found coin-shaped lesions by slit-lamp biomicroscopy in all patients (8/8; 100%) and suggested that the lesions are a characteristic sign of CMV corneal endotheliitis.[6] However, we detected coin-shaped lesions in only 1 patient (16.7%) at the first visit. At subsequent follow-up visits, 2 additional patients had coin-shaped lesions (Figure 1; total, 3/6; 50%). The coin-shaped lesions were not detectable in the remaining 3 patients throughout the follow-up visits. Considering that we could visualize owl eye morphologic features in all patients (6/6; 100%), the presence of not only coin-shaped lesions by slit-lamp biomicroscopy, but also of owl eye morphologic features by HRT2-RCM may be useful as an adjunct method for the noninvasive diagnosis of CMV corneal endotheliitis. For example, owl eye morphologic features may indicate that ganciclovir treatment should be initiated soon after the confocal examination under ten-

precipitates in the peripheral cornea were observed. Sectorial edemas from the periphery to the center were detected under fluorescein staining (arrowheads). (Top right) Epithelial basal cell layer in the center of the cornea demonstrating normal results by Heidelberg Retina Tomograph 2 Rostock Cornea Module (HRT 2-RCM). Bar = 50 μm. (Second row left) Seemingly normal Bowman layer with minimal highly reflective tiny dots. Nerves were not detectable. (Second row middle) Subepithelial opacity with increased reflectivity of keratocytes was observed. (Second row right) Highly reflective dots and needle-shaped bodies (arrows) were noted. (Third row left) HRT 2-RCM identified large endothelial cells whose nuclei had a high reflection area surrounded by a halo of low reflection, which resembled an owl eye (arrows). Endothelial cell density was 692 cells/mm^2. (Third row middle) Multiple intranuclear inclusion bodies in a cartwheel arrangement were seen in large cells (arrow). (Third row right) Further owl eye morphologic features were noted during the subsequent follow-up visit (arrows). (Bottom left) Sequential image of Third row right, 4 μm forward from the anterior chamber. Highly reflective round bodies were noted, which presumably show necrotic and protruded owl eye cells identified in Third row right (arrows). (Bottom middle) Owl eye morphologic features in a different location (arrows). (Bottom right) Sequential image of Bottom middle, 6 μm forward toward the anterior chamber. Highly reflective round bodies, presumably the identical cell of owl eye morphologic features seen in the Bottom middle were noted (arrows).